

A parametric study on the dynamic behavior of porous bronze at various strain rates

Yue Zhang¹ · Jianxing Hu¹ · Jianyin Lei¹ · Zhihua Wang¹ · Longmao Zhao¹

Received: 11 July 2016 / Accepted: 12 September 2016 / Published online: 17 September 2016
© Springer-Verlag Berlin Heidelberg 2016

Abstract An experimental investigation on the porous bronze at various strain rates is firstly carried out in this study to explore the effects of relative density and strain rate in the mechanical behavior. Furthermore, a multi-parameter constitutive model of describing the rate-dependent behavior for porous bronze is developed. The parameters in the constitutive model are density dependent, and the specific forms of these parameters as functions of relative density are obtained. It can be concluded from the test results and constitutive model that the high relative density leads to increase in yield strength and energy absorption capacity of the materials and the strain rate also has positive effects on the yield strength and energy absorption capacity of porous bronze.

1 Introduction

There have been generally three categories of solid materials (i.e., the low relative density solids, high relative density solids and medium relative density solids) in industrial application. The low porosity solids contain the solids that are in the traditional sense, which are with high relative density (normally beyond 99 %). The relative density of low relative density solids is typically below 30 %, such as woods and artificial cellular and foam materials. These materials have been a critical candidate for protective structural used in industry such as automotive, railways and

aerospace. The wide range of application of porous materials has interested researchers, so the studies on the mechanical behavior of porous materials at various strain rates have been extensively undertaken [1–5].

In order to meet the requirement for both the strength and energy absorption capacity in practical engineering application, like the seats of airplane, the medium relative density solids, whose relative densities are from 30 to 90 %, have been fabricated. Some recent studies about artificial heavy porous metals (such as porous bronze) have been reported: Wang et al. [6] studied the behavior of porous iron and bronze under quasi-static loading and at low strain rate (10/s) condition, and they also investigated the effect of powder size in sintering process on compressive behavior of porous copper, which indicated the effect of porosity on modulus, yield strength and deformation mechanism of the material in quasi-static test [7, 8]. They considered that there existed obvious strain hardening in behavior of porous iron and bronze, and the effect of strain rate on dynamic behavior of porous bronze was evident [9, 10]. The effects of porosity and loading rate on yield stress, energy absorption and load carrying capacity of porous bronze and porous iron were reported in [11, 12]. Song and Tane et al. [13–16] investigated the effect of temperature and strain rate on behavior of porous materials and compared the load carrying capacity of porous materials which they fabricated with that of aluminum foams. In the above articles, the compressive stress level of porous bronze exhibits the sensitivity of strain rate. However, high strain rate may produce lower stress of porous bronze, which was reported in [17], and Wang et al. [18] declared that strain rate has no effect on the strength of porous bronze. Furthermore, there is not yet a good understanding of the constitutive models for these porous metals with medium–high relative density.

✉ Zhihua Wang
wangzh@tyut.edu.cn

¹ Institute of Applied Mechanics and Biomedical Engineering,
Taiyuan University of Technology, Taiyuan 030024,
People's Republic of China

It is important to obtain mechanical properties of medium porosity solids from a single constitutive model which is able to describe the behavior at a wide range strain rates of specific porous metals with different densities. Such data are essential in realistic numerical simulations for the industrial design of structures because many engineering structures may be subjected to complex loadings in service.

In this study, the behavior of the porous bronze under quasi-static and dynamic loadings was researched systematically. The experimental investigations on the mechanical properties at various strain rates of the porous bronze with different relative densities were firstly carried out to explore the effects of relative density and strain rate. Moreover, a multi-parameter constitutive model that can fully describe the compressive behavior of porous bronze was developed based on experimental results, and the dependency of the model parameters on the relative densities of materials was determined.

2 Experimental study

2.1 Material and sample

The porous bronze was fabricated by powder metallurgy process under argon gas. As for the chemical composition, Al and Sn account for 0.4 and 11.07 % of the entire mass of porous bronze, while the Cu is the base material.

Due to the porous structure, attention is required in deciding the size of samples in order to guarantee good reliability in measurement. It was suggested that the size of sample should be 10–20 times as much as the pore size [19]. Examination of the microstructure was carried out by utilizing optical microscopy. The average pore sizes of the porous bronze are approximately 50–400 μm for different relative densities, as listed in Fig. 1. Therefore, the porous bronze was cut into cylinders with sizes of $\phi 25 \times 10$ mm for dynamic testing. Before testing, each specimen was weighed to calculate their relative densities. Their respective relative densities of the porous bronze are 60, 63.5, 69, 75 and 77.5 %.

2.2 Experiments and results

To ensure the reliability of test results, quasi-static or dynamic compressions were tested repeatedly at least three times for each relative density of the porous bronze. The force–displacement data were obtained from universal material machine, which then was converted to stress–strain data at a strain rate of 0.001/s. Figure 2 demonstrates the mechanical behavior of porous bronze with different relative density under quasi-static condition.

Dynamic tests were performed on the samples by split Hopkinson pressure bar (SHPB) [20, 21], as shown in

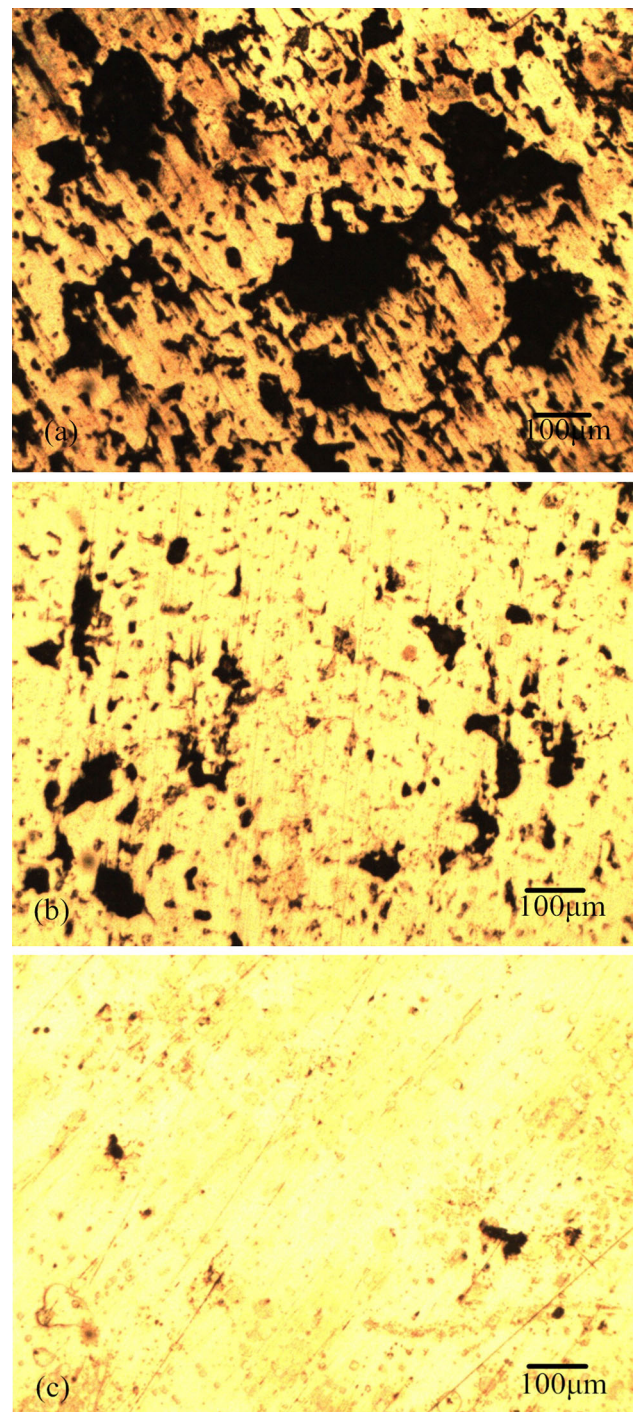


Fig. 1 Micrograph ($\times 100$) vertical sectioning of undeformed porous bronze with different relative densities: **a** 60 %; **b** 69 %; **c** 77.5 %

Fig. 3. The striker, incident bar and transmitter bars with the respective lengths of 800, 2000 and 2000 mm are made of high-strength steel, while the diameter is identical (37 mm). The specimen is sandwiched between incident bar and transmitter bar. To reduce the friction effect, grease was concatenate with samples, the end surfaces of incident and transmitter bars and also used between bars and pillow

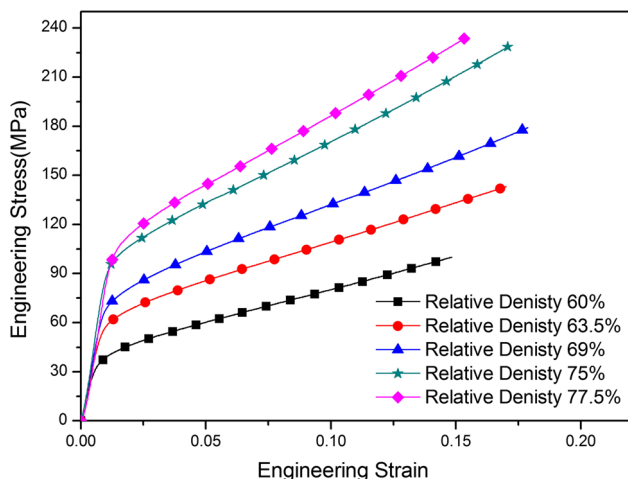


Fig. 2 Behavior of porous bronze under quasi-static loading

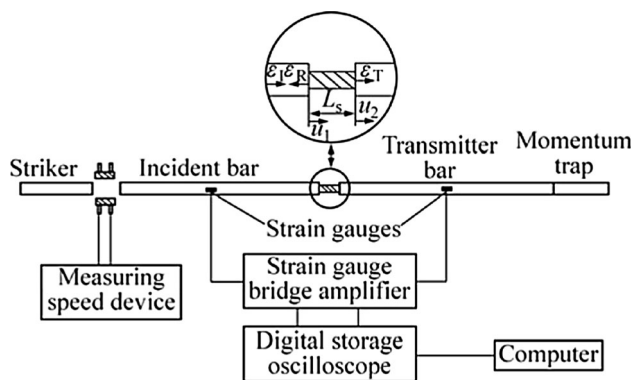


Fig. 3 Schematic diagram of split Hopkinson pressure bar

blocks that support the bars. A compression wave was generated when the coaxial impact of striker and incident occurred. Then, a part of stress wave reflected after the compression wave reaching the interface between specimen and incident bar. The other portion of the stress wave transmitted through the specimen and the transmitter bar. The incident pulse and reflect wave which propagated in the incident bar can be captured by the strain gauges attached to the middle of the incident bar. Like incident pulse and reflect wave, the transmitted wave was captured by the strain gauges but attached to the middle of the transmitter bar. The original record of incident wave, reflect wave and transmitted wave can be seen in Fig. 4.

The compressive stress–strain curves of these materials and average strain rates can be determinate based on the records of transmitted and reflected waves, respectively. The compressive stress–strain curves of the porous bronze with different relative densities at various strain rates (600/s, 900/s and 1500/s) are shown in Figs. 5 and 6, which reveal that strain rate has a positive effect on yield strength of the porous bronze. It should be noted that the relative density also has an impact on the mechanical behavior of

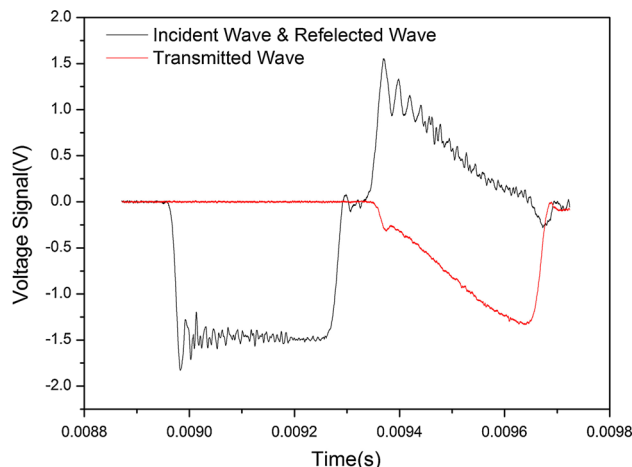


Fig. 4 Original record of incident, reflected and transmitted waves

these materials under whether quasi-static or dynamic condition, i.e., the porous bronze with larger relative density possess the higher yield strength.

3 Constitutive model

It is well-known that the constitutive model is a theoretical tool to quantificationally characterize the mechanical behavior for materials. Therefore, a full mathematical description for the rate-dependent behaviors of porous metal at various strain rates is meaningful for the corresponding impact events. According to the suitable constitutive model, researchers could investigate the practical engineering problems by finite element method. However, the constitutive models recently presented only based on the stress–strain curves under quasi-static loading.

In this paper, due to the complexity of the constitutive models based on deformation mechanism applied in industry, only a multi-parameter empirical constitutive model was proposed to depict the entire compressive behavior of porous bronze with different relative densities under both quasi-static and dynamic conditions. In this constitutive model, the uniaxial compressive stress σ is given by:

$$\sigma = \left(A(\hat{\rho}) \frac{e^{\alpha(\hat{\rho})\varepsilon} - 1}{1 + e^{\beta(\hat{\rho})\varepsilon}} \right) \left(1 + B(\hat{\rho}) \lg \frac{\dot{\varepsilon}}{\dot{\varepsilon}_0} \right) \quad (1)$$

where ε is the compressive strain; $\hat{\rho} = \rho^*/\rho_s$ is the relative density of the porous bronze, where ρ^* is the density of specimen and ρ_s is the density of matrix material; $\dot{\varepsilon}$ is the average strain rate and $\dot{\varepsilon}_0$ is reference strain rate which was set as 0.001/s here. The first term of Eq. (1) is used to describe the universal deformation of porous bronze, and the second term is used to represent the effect of the strain rate. The parameters A , α , β and B can characterize the

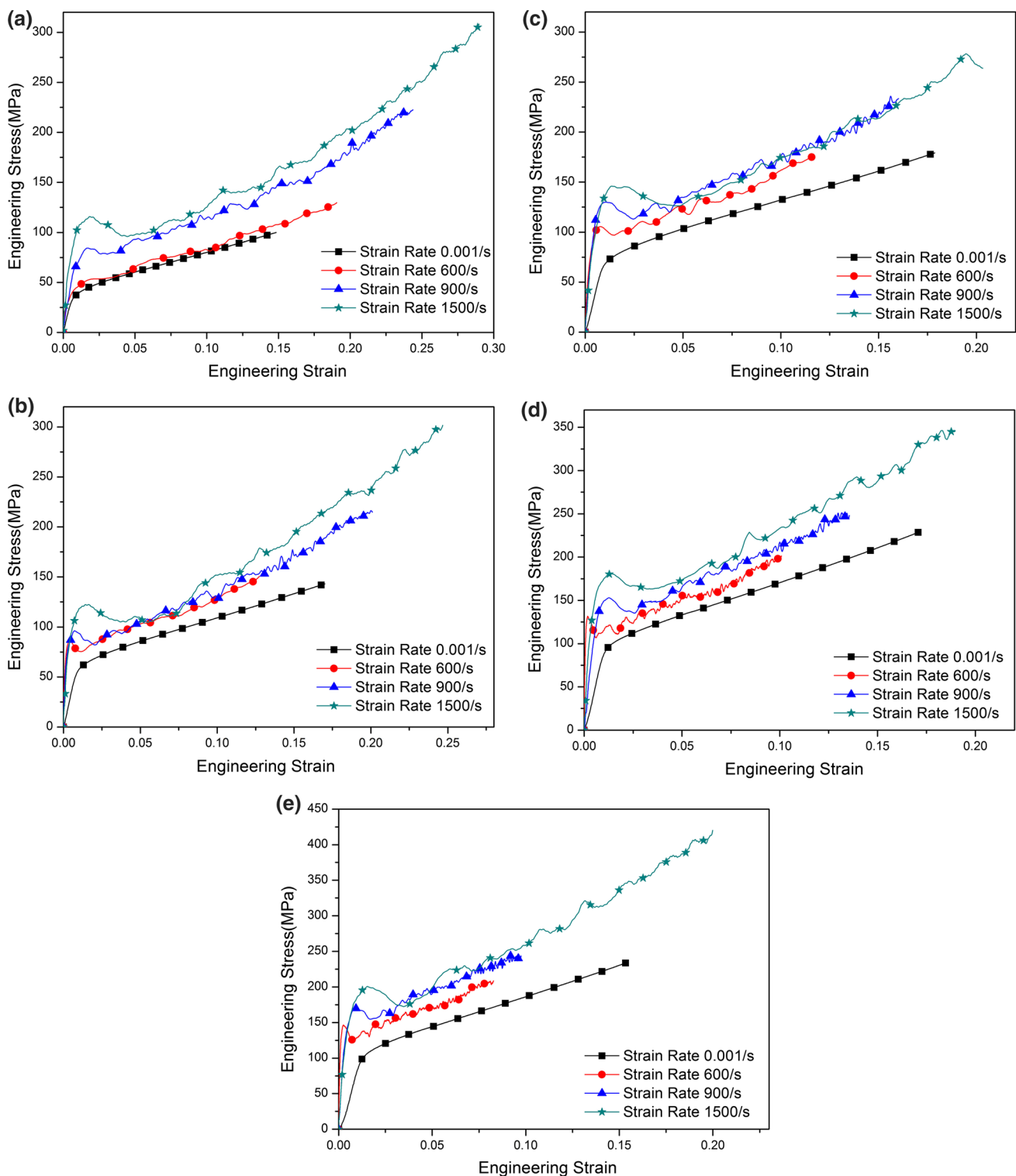


Fig. 5 Behavior of porous bronze at various strain rates: **a** with relative density 60 %; **b** with relative density 63.5 %; **c** with relative density 69 %; **d** with relative density 75 %; **e** with relative density 77.5 %

primary features of the behavior under different loadings. For instance, parameter A can represent the compressive yield stress under quasi-static condition. Parameters α and β simultaneously represents the plastic response of porous

bronze. The last parameter B represents the dependence of strain rate. The details of every parameter can be found in [22]. The number of parameters used in function in Eq. (1) is only four to minimize the difficulty in utilizing this

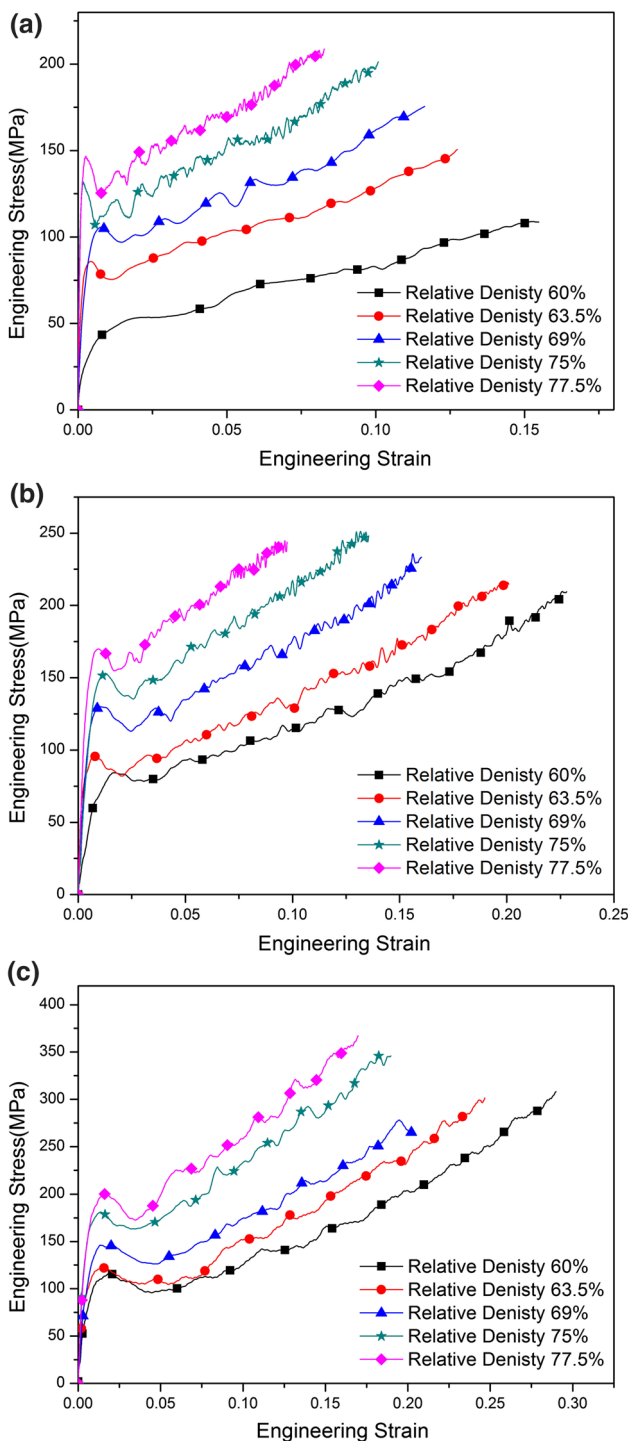


Fig. 6 Behavior of porous bronze with different relative densities: **a** at strain rate 600/s; **b** at strain rate 900/s; **c** at strain rate 1500/s

function, and this function is continuously differentia, i.e., no singularity in the entire domain.

Figure 7 shows the effects of the various values of all these parameters on the entire stress–strain curves described by the constitutive model, where the parameter A is set as a constant of 40.

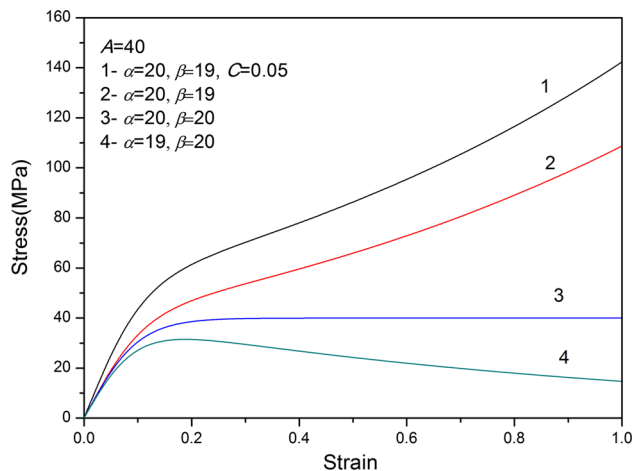


Fig. 7 Illustration of model for various parameters

4 Discussion

4.1 The correction of wave dispersion

In this paper, the SHPB with $\phi 37$ mm was used in dynamic tests. It is important that the wave dispersion should be corrected referring to [23]. Therefore, the Fourier transform procedure [24] was carried out to correct the wave dispersion of the dynamic data. Figure 8a, b shows the correction of reflect wave and transmitted wave, and Fig. 8c shows the comparison between the measured strain–stress curve and corrected curve. The largest error is no more than 5 %, and there is only little difference between the yield stress of measured strain–stress curve and corrected strain–stress curve. Therefore, the wave dispersion in wave propagation can be neglected in the bars with size of $\phi 37$ mm in case of this paper.

4.2 Yield stress

Because there do not exist an obvious yield stage in the behavior of porous bronze, the yield stress is represented by the 0.2 % proof stress that can be calculated from the experimental data. Then, the 0.2 % proof stress is normalized by the 0.2 % proof stress of porous bronze with the maximum relative density (77.5 %) under quasi-static loading, to explore the effect of relative density and the strain rate sensitivity on yield stress of the materials.

Figure 9 shows the effect of relative density and strain rate on the yield strength of the porous bronze. It is obvious that the porous bronze with higher relative density possess higher yield strength, i.e., relative density has a positive effect on the yield strength of these materials. Meanwhile, it is observed that strain rate, like relative density, has a positive effect on the yield strength of these materials. Therefore, it can be drawn that the yield strength of the porous bronze is sensitive to the strain rate.

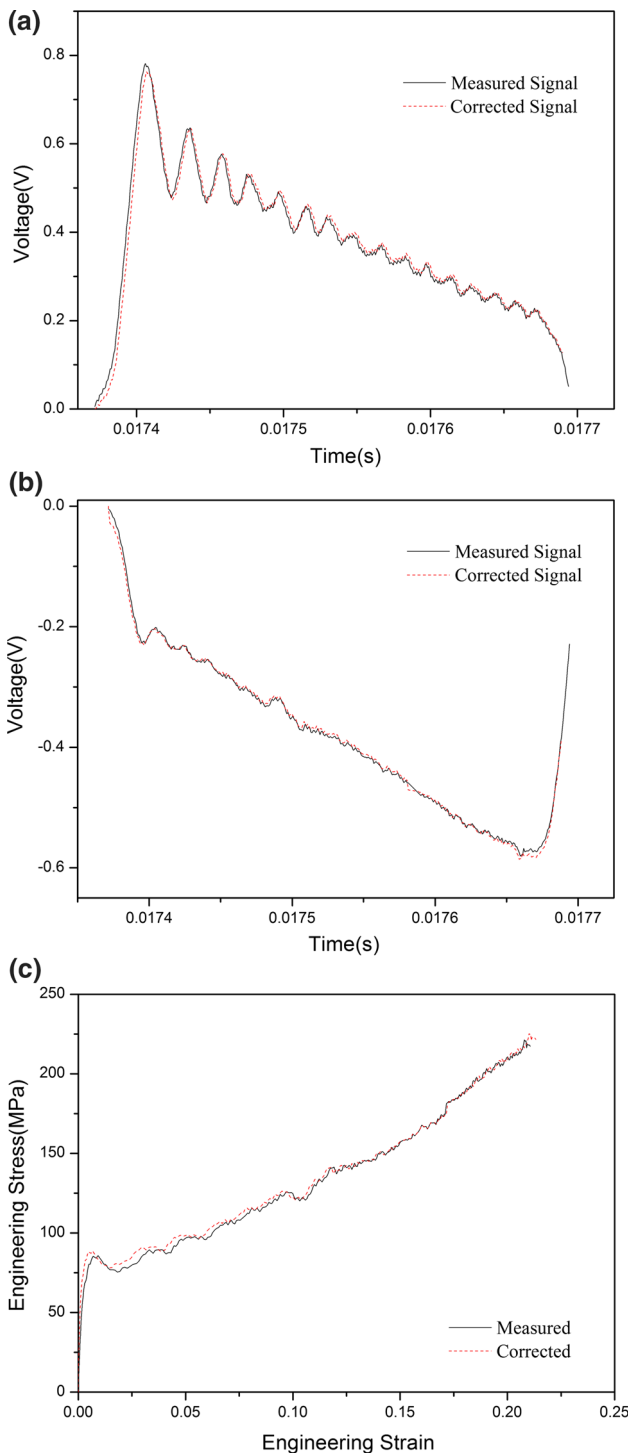


Fig. 8 Comparison of measured curves and corrected curves: **a** reflected wave; **b** transmitted wave; **c** stress–strain curve

4.3 Energy absorption

Energy absorption capacity is defined as the capability of the material for absorbing energy while experiencing large deformation or brittle fracture. The energy absorption per

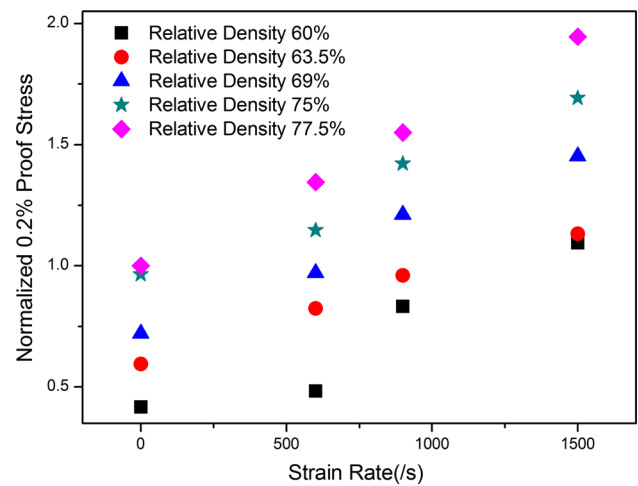


Fig. 9 Normalize yield stress of porous bronze

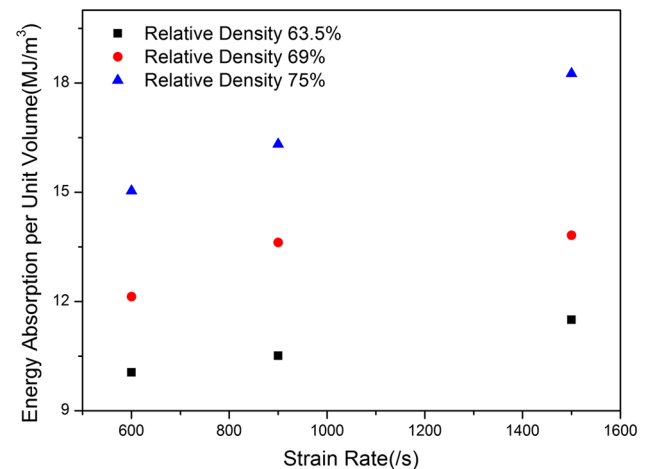


Fig. 10 Energy absorption per unit volume for porous bronze compressed up to 10 % strain

unit volume can be obtained by calculating the area under stress–strain curve.

$$W = \int_0^\epsilon \sigma d\epsilon \tag{2}$$

The energy absorption per unit volume for porous bronze were calculated for the same level of strain (10 %) [11] and shown in Fig. 10. It can be observed that energy absorption per unit volume for porous bronze at higher strain rate is higher, so the energy absorption per unit volume is strain rate sensitive. It also shows increasing tendency of energy absorption per unit volume with relative density.

4.4 Parameters of constitutive model

Although there are four parameters in this constitutive model, determining the parameters that can describe

Table 1 Value of parameters A , α and β with different relative densities

	Relative density 60 %	Relative density 63.5 %	Relative density 69 %	Relative density 75 %	Relative density 77.5 %
A	41.72	59.57	72.12	92.11	100.06
α	298.0696	279.6605	257.3510	248.4615	224.2611
β	291.8111	274.0972	251.8823	242.7743	217.7489

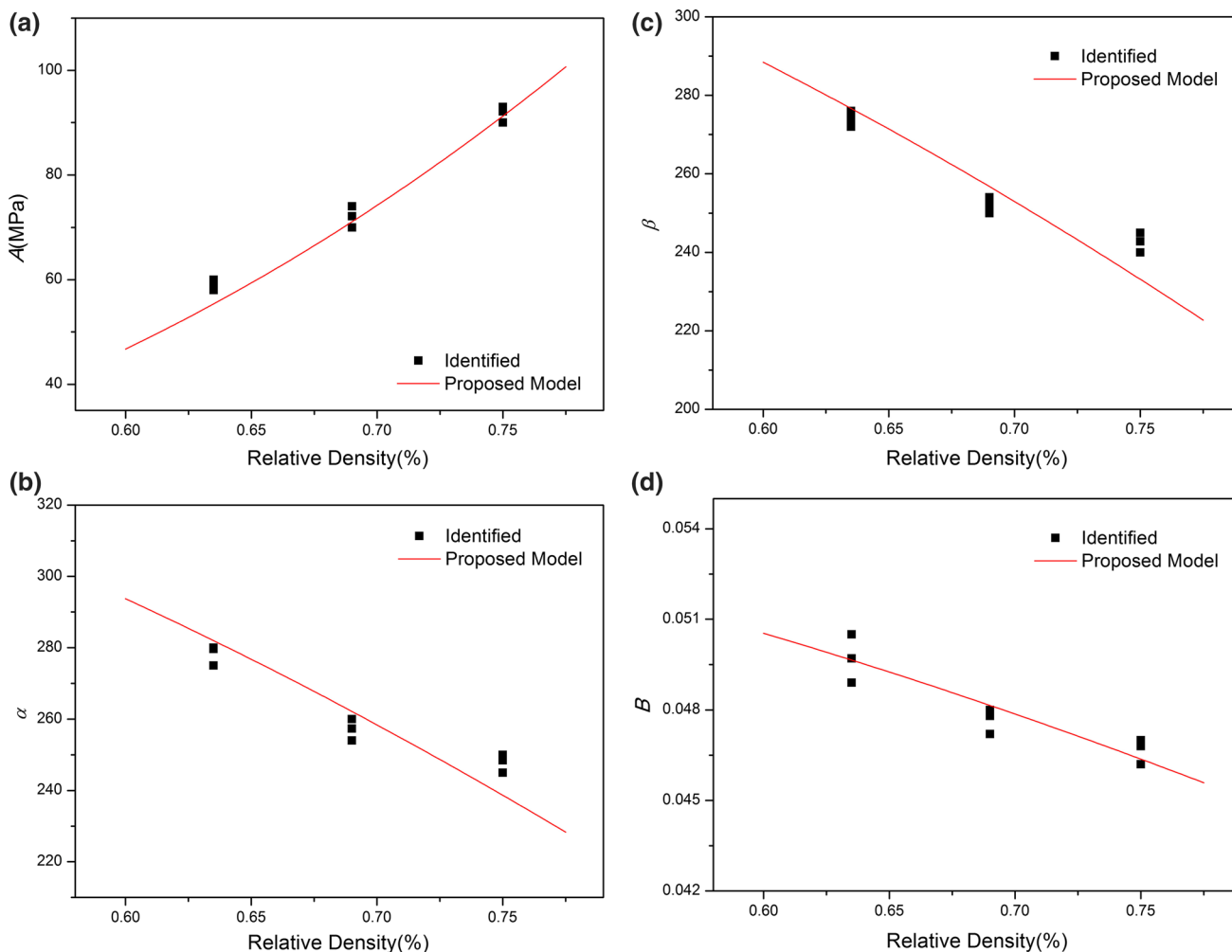


Fig. 11 Functional relationship of model parameters A (a), α (b), β (c) and B (d) determined in terms of relative density

experimental compressive behavior of porous bronze was not trivial in this work. The nonlinear optimization procedure was performed firstly to fit the experimental data. This function employed a Gauss–Newton iterative algorithm to minimize the mean squared error between the experimental data and the prediction of the function. Utilizing the first term in Eq. (1), the value of a convergent parameter set (A , α and β) can be obtained. Then, the value of parameters A , α and β and the data of dynamic experiments were used to acquire the value of parameter B . Finally, the functional form of the uniaxial compressive stress σ only

in terms of compressive strain, initial relative density and strain rate was obtained by using all the above-determined parameters. Table 1 shows the value of parameters with different relative density at various strain rates.

The functional forms of the parameters in this model were determined in terms of relative density of the porous bronze based on the value of parameters obtained above, as shown in Fig. 11. According to the trends that were observed from Fig. 11, a serial functions were chosen to establish the relationship between the relative density $\hat{\rho}$ and the parameters A , α , β and B .

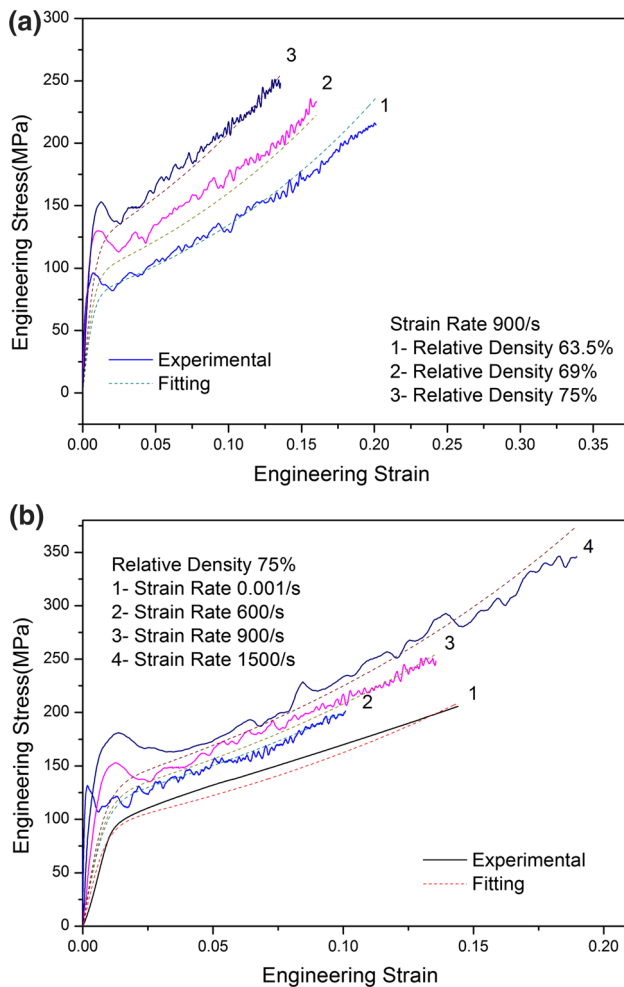


Fig. 12 Experimental and fitting stress–strain curves of porous bronze: **a** with the different relative densities; **b** at different strain rates

$$A = 216.3\hat{\rho}^3 \quad (3)$$

$$\alpha = -271.9\hat{\rho}^2 + 391.6 \quad (4)$$

$$\beta = -273.1\hat{\rho}^2 + 386.8 \quad (5)$$

$$B = -0.0205\hat{\rho}^2 + 0.0579 \quad (6)$$

Figure 11a and Eq. (3) show the effect of relative densities of these materials on the parameter A . It is distinct that the value of parameter A , which was used to represent the compressive strength of material increases with respect to relative density. Conversely, the value of parameters α and β shows a decreasing tendency with increasing relative density according to Fig. 11b, c and Eqs. (4, 5). However, the value of parameter α is always larger than that of parameter β no matter how the relative density changes, which means the relative density does not affect on the hardening-like response of the porous bronze. Likewise, the value of parameter B with lower relative density is

larger than those with higher relative densities, which can be seen in Fig. 11d and Eq. (6). Therefore, strain rate might have a stronger effect on the behavior of porous bronze with lower relative density.

Comparison between the experimental results and the prediction of model by using Eqs. (3–6) with different relative densities and strain rates was made in Fig. 12. It can be seen that a good agreement is observed between the prediction of model and experimental results. Especially, the quality of the fitting is remarkable in the elastic region under quasi-static loading.

5 Conclusions

Porous bronze with different relative densities (60–77.5 %) was investigated at various strain rates by quasi-static tests and split Hopkinson pressure bar tests. A multi-parameter phenomenological constitutive model that is able to depict the entire stress–strain curves of porous bronze at various strain rates was further developed. The comparison of experimental data and the predictions of the model demonstrated the validity of this model. Following conclusions can be drawn from the experimental and analytical work carried out in the present study:

1. Relative density affects the properties of porous bronze. The yield strength and energy absorption capacity of this material rise in terms of the increasing relative density.
2. The strain rate has an effect on the behavior of porous bronze. The compressive stress and energy absorption capacity of the bronze are higher with the higher strain rate, which is an important fact needed to be considered for application.
3. The parameters in the constitutive model are density dependent, and the specific forms of these parameters as functions of relative density are obtained, which might be responsible for the changes in yield stress and the hardening-like behavior of porous bronze.

Acknowledgments This work is supported by the National Natural Science Foundation of China (Grant No. 11172196), Shanxi Scholarship Council of China (2013-046), the Top Young Academic Leaders of Shanxi and the Outstanding Innovative Teams of Higher Learning Institutions of Shanxi. The financial contributions are gratefully acknowledged.

References

1. Z.H. Wang, J.H. Shen, G.X. Lu, L.M. Zhao, Compressive behavior of closed-cell aluminum alloy foams at medium strain rates. *Mater. Sci. Eng. A* **528**, 2326–2330 (2011)

2. Z.W. Zhou, Z.H. Wang, L.M. Zhao, X.F. Shu, Loading rate effect on yield surface of aluminum alloy foams. *Mater. Sci. Eng. A* **543**, 193–199 (2012)
3. Z.W. Zhou, Z.H. Wang, L.M. Zhao, X.F. Shu, Uniaxial and biaxial failure behaviors of aluminum alloy foams. *Compos. B* **61**, 340–349 (2014)
4. L. Jing, Z.H. Wang, L.M. Zhao, The dynamic response of sandwich panels with cellular metal cores to localized impulsive loading. *Compos. B Eng.* **94**, 52–63 (2016)
5. L. Jing, Z.H. Wang, J.G. Ning et al., The dynamic response of sandwich beams with open-cell metal foam cores. *Compos. Part B Eng.* **42**(1), 1–10 (2011)
6. B. Wang, J.R. Klepaczko, G. Lu, L.X. Kong, Viscoplastic behavior of porous bronze and irons. *J. Mater. Process. Technol.* **113**, 574–580 (2001)
7. E. Zhang, B. Wang, On the compressive behaviour of sintered porous coppers with low to medium porosities—part I: experimental study. *Int. J. Mech. Sci.* **47**, 744–756 (2005)
8. B. Wang, E.L. Zhang, On the compressive behavior of sintered porous coppers with low-to-medium porosities—part II: preparation and microstructure. *Int. J. Mech. Sci.* **50**, 550–558 (2008)
9. B. Wang, J. Zhang, G. Lu, Taylor impact test for ductile porous materials—part 2: experiments. *Int. J. Impact Eng.* **28**, 499–511 (2003)
10. G. Lu, B. Wang, T.G. Zhang, Taylor impact test for ductile porous materials—part 1: theory. *Int. J. Impact Eng.* **25**, 981–991 (2001)
11. N. Iqbal, P. Xue, H.J. Liao, B. Wang, Y.L. Li, Material characterization of porous bronze at high strain rates. *Mater. Sci. Eng. A* **528**, 4408–4412 (2011)
12. P. Xue, N. Iqbal, H.J. Liao, et al. Experimental study, on strain rate sensitivity of ductile porous irons. *Int. J. Impact Eng.* 2011: 1–5
13. M. Tane, Y.H. Song, H. Nakajima, Formation mechanism of a plateau stress region during dynamic compression of porous iron: interaction between oriented cylindrical pores and deformation twins. *Mater. Sci. Eng. A* **591**, 150–158 (2014)
14. Y.H. Song, M. Tane, H. Nakajima, Dynamic and quasi-static compression of porous carbon steel S30C and S45C with directional pores. *Mater. Sci. Eng. A* **534**, 504–513 (2012)
15. Y.H. Song, M. Tane, H. Nakajima, Appearance of a plateau stress region during dynamic compressive deformation of porous carbon steel with directional pores. *Scr. Mater.* **64**, 797–800 (2011)
16. Y.H. Song, M. Tane, H. Nakajima, Peculiar formation mechanism of a plateau stress region during dynamic compressive deformation of porous carbon steel with oriented cylindrical pores. *Acta Mater.* **60**, 1149–1160 (2012)
17. J. Zhang, L. Zhao, G. Lu, etc. High strain rate behavior of porous materials made of bronze and iron alloys. in Proceedings of 8th International Symposium on IMPLAST2003, pp. 333–342
18. Q.Z. Wang, D.M. Lu, C.X. Cui et al., Compressive behaviors and energy-absorption properties of an open-celled porous Cu fabricated by replication of NaCl space-holders. *J. Mater. Process. Technol.* **211**, 363–367 (2011)
19. A.E. Simone, L.J. Gibson, Aluminum foams produced by liquid-state processes. *Acta Mater.* **46**(9), 3109–3123 (1998)
20. B.A. Gama, S.L. Lopatnikov, J.W. Gillespie, Hopkinson bar experimental technique: a critical review. *Appl. Mech. Rev.* **57**(4), 223–250 (2004)
21. Z.H. Wang, H.W. Ma, L.M. Zhao, G.T. Yang, Studies on the dynamic compressive properties of open-cell aluminum alloy foam. *Scr. Mater.* **54**(1), 83–87 (2006)
22. Z.H. Wang, L. Jing, L.M. Zhao, Elasto-plastic constitutive model of aluminum alloy foam subjected to impact loading. *Trans. Nonferr. Met. Soc. China* **21**, 449–454 (2011)
23. Y.G. Wang, L.L. Wang, Stress wave dispersion in large-diameter SHPB and its manifold manifestations. *J. Beijing Inst. Technol.* **13**, 247–253 (2004)
24. P.S. Follansbee, C. Frantz, Wave propagation in the split Hopkinson pressure bar. *J. Eng. Mater. Technol.* **105**, 61–66 (1983)